Journal of Advanced Biomedical Sciences

Journal of Advanced Biomedical Sciences
https://jabs.fums.ac.ir/
Online ISSN: 2783-1523

Fasa University of Medical Sciences

Inhibitory Potential of Benzo[a]phenazin-5-ol Derivatives Against C-Kit Kinase: Molecular Docking and Prediction of ADME/Drug-Likeness Properties

Abolfazl Olyaei[1], Monir Shalbafan[1], Fatemeh Rahimi[1], Mahdieh Sadeghpour[2]

1. Department of Chemistry, Faculty of Science, Imam Khomeini International University, Qazvin, Iran
2. Department of Chemistry, Qazvin Branch, Islamic Azad University, Qazvin, Iran

Article Info

Article Type:
Research Article

Article history:
Received
05 May 2024
Received in revised form
17 May 2024
Accepted
09 Jun 2024
Published online
14 Jun 2024

Publisher
Fasa University of Medical Sciences

Abstract

Background & Objectives: C-Kit, a receptor tyrosine kinase involved in intracellular signaling, has a mutated form that significantly contributes to the development of certain cancers. This study aimed to evaluate a series of benzo[a]phenazin-5-ol-tethered tri-substituted methane derivatives as potential pharmacophores for inhibiting C-Kit kinase.

Materials & Methods: Benzo[a]phenazine-5-ol derivatives were sketched and converted into Mol2 files using Marvin software. Their three dimensional (3D) structures were generated and saved in PDB format. Molecular docking studies with the C-Kit kinase (PDB code 1t46) were performed using AutoDock 4.2. Additionally, the derivatives' physicochemical properties, ADME characteristics, and drug-likeness parameters were assessed with the SwissADME online tool.

Results: Molecular docking studies of benzo[a]phenazin-5-ol derivatives (**A-L**) against C-kit kinase revealed that compounds **A** and **C** exhibited greater selectivity and stronger inhibitory effects than the reference drug, Sunitinib. Ligplot analysis demonstrated that compound **A** formed four hydrogen bonds with Arg791(A), Ile789(A), and His790(A), while compound **C** formed two hydrogen bonds with Ile571(A) and Ile789(A). ADME analysis indicated that all compounds, except **C**, **D**, and **I**, are potential P-gp substrates. Drug-likeness analysis showed one or two violations of Lipinski's rule of five.

Conclusion: In summary, molecular docking studies identified compounds **A** and **C** as promising lead candidates for inhibiting C-kit kinase, demonstrating superior binding to the active site compared to Sunitinib. ADME and drug-likeness analysis revealed that compound **A** is a potential P-gp substrate with one violation of Lipinski's rule of five, making it the closest pharmacological match to Sunitinib and a strong candidate for further investigation.

Keywords: benzo[a]phenazin-5-ol, molecular docking, C-Kit kinase, Auto Dock 4.2, drug-likeness

Cite this article: Olyaei A, Shalbafan M, Rahimi F, Sadeghpour M. Inhibitory Potential of Benzo[a]phenazin-5-ol Derivatives Against C-Kit Kinase: Molecular Docking and Prediction of ADME/Drug-Likeness Properties. J Adv Biomed Sci. 2024; 14(3): 222-231.
DOI: 10.18502/jabs.v14i3.16359

Introduction

Phenazine systems represent an important class of aza-polycyclic compounds readily found in nature, with benzo[a]phenazine being a notable derivative. These compounds have garnered significant interest due to their role as structural subunits in various important natural products and their diverse biological properties, including antifungal (1), anti-tumor (2), trypanocidal (3), and dual inhibitory effects

Corresponding Author: Abolfazl Olyaei, Department of Chemistry, Faculty of Science, Imam Khomeini International University, Qazvin, Iran.
Email: Olyaei_a@sci.ikiu.ac.ir

[Downloaded from jabs.fums.ac.ir on 2026-11-10]

[DOI: 10.18502/jabs.v14i3.16359]

on topoisomerase I and II, making them valuable as antitumor agents (4). It is worth noting that the literature documents relatively few methods for synthesizing benzo[a]phenazin-5-ol-tethered tri-substituted methanes (5-11), among which hydroxybenzo[a]phenazinepyrazol-5(4H)-one derivatives (9) have demonstrated anticancer and antimicrobial activities. Tyrosine kinases, enzymes that selectively phosphorylate tyrosine residues within specific proteins, play a crucial role in modifying signaling cascades, thereby influencing cell growth, differentiation, migration, apoptosis, and death. C-Kit, classified as a type III receptor tyrosine kinase (RTK), has been implicated in cancer development (12). Currently recognized primarily as a stem cell factor (SCF), C-Kit is actively involved in critical functions within the human body, including fertility, homeostasis, and melanogenesis (13, 14). The deregulation of C-Kit, encompassing overexpression and gain-of-function mutations, has been identified in various human cancers, with leukemia representing the initial cancer type associated with activating mutations in C-Kit (15). Furthermore, Kit mutations have been detected in cancers such as unilateral ovarian dysgerminoma (16-18), melanoma (19), and others (20-22).

Cancer growth is typically facilitated by the activation of mutations or gene amplifications in specific serine or tyrosine kinases. Tyrosine kinase inhibitors, such as Imatinib, Axitinib, Nilotinib, Gefitinib, Sunitinib, and Dasatinib, fall into two classes: small molecules targeting specific kinases and monoclonal antibodies targeting either receptor kinases or their ligands (23). In this study, Sunitinib serves as a standard drug for comparing its activity with benzo[a] phenazin-5-ol-tethered tri-substituted methane derivatives acting as C-kit inhibitors. Sunitinib functions as a multitargeted receptor tyrosine kinase inhibitor, targeting Platelet-derived growth factor receptors (PDGF-R)-α and β, FMS-like tyrosine kinase 3, vascular endothelial growth factor receptor (VEGFR)-1, -2, and -3, colony-stimulating factor 1 receptor, and glial cell-line derived neurotrophic factor receptor (24, 25). It is employed in the treatment of renal cell carcinoma and gastrointestinal stromal tumors (26). Molecular docking, a structure-based computational method, generates binding modes and affinities between ligands and targets by predicting their interactions (27, 28). It has become an invaluable tool supporting diverse areas of drug discovery (29), with applications in virtual screening, target fishing, drug side effect prediction, polypharmacology, and drug repurposing. Computer-assisted computations of ADME (Absorption, Distribution, Metabolism, and Excretion) properties of drugs are increasingly considered as an anticipatory and reliable complement to experimental approaches. It is crucial to study the ADME properties and other drug-likeness characteristics of molecules before their use as pharmaceutical aids. ADME studies in the early stages of drug discovery can help reduce pharmacokinetics-related failures during clinical phase trials. The SwissADME web tool is an effective resource for predicting physicochemical parameters that correlate with *in vitro*, *in vivo*, and *in silico* investigations (30). The aim of this study is to elucidate the binding mode, affinity, and potential inhibitory activity of benzo[a]phenazin-5-ol derivatives against C-kit kinase through molecular docking and prediction of ADME/drug-likeness properties. The selection of C-kit kinase for molecular docking of benzo[a]phenazin-5-ol derivatives as inhibitors is supported by recent research demonstrating the anti-tumor activity of these compounds, as evidenced in various articles.

Material and Methods

The structures of benzo[a]phenazine-5-ol derivatives were sketched, drawn, and their Mol2 files generated using Marvin software. Subsequently, three dimensional (3D) structures were created, and the molecules were converted

[Downloaded from jabs.fums.ac.ir on 2026-11-10]
[DOI: 10.18502/jabs.v14i3.16359]

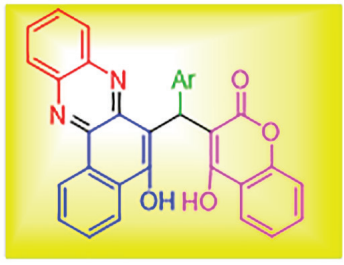
into PDB format. An appropriate force field was applied, followed by optimization using Chimera software (version 1.17.1). Ligand structures were prepared using AutoDock Tools software (version 1.5.6) by incorporating polar hydrogens and assigning Kollman charges, then saved in PDBQT format. The C-Kit kinase structure of interest (PDB code 1t46) was prepared by eliminating water molecules and other heteroatoms, introducing polar hydrogens, and allocating Gasteiger charges to protein atoms. The resulting protein structure was saved in PDBQT format. Grid box dimensions were adjusted to encompass the protein's binding site, with a grid size of 70×70×70 xyz points, grid spacing of 0.375 Å, and grid center designated at dimensions (x, y, and z): 27.696, 26.657, and 39.342. Docking was carried out using the Lamarckian Genetic Algorithm (LGA), employing a population size of 150 individuals, a maximum of 2.5 million energy evaluations, a maximum of 27,000 generations, a mutation rate of 0.02, and a crossover rate of 0.8. Docking simulations were executed on a high-performance computing cluster utilizing multiple processors. Each ligand was individually docked into the protein structure, and the most promising docked runs were selected for further analysis.

Binding energies of the docked compounds were determined using the AutoDock scoring function, which considers van der Waals interactions, hydrogen bonding, and electrostatic interactions between the ligand and the protein. Clusters were created using a root-mean-square deviation (RMSD) tolerance of 0.5 Å, and subsequent analysis focused on the top 10 clusters exhibiting notable negative binding energies. Ligplot software (version 2.2) was employed to visualize the binding modes of ligands within these prominent clusters. In silico ADME screening and drug-likeness evaluation were conducted using the SwissADME web tool, developed by the Swiss Institute of Bioinformatics. Compounds with high-ranking binding energy scores were selected for further screening. Basic physicochemical properties, including molecular weight (MW), molecular refractivity (MR), atom counts, and polar surface area (PSA), were calculated using OpenBabel, version 2.3.0 (31). Abbott Bioavailability scores were calculated to estimate the likelihood of a compound having at least 10% oral bioavailability, based on its total charge, TPSA, and any deviations from Lipinski's rule of five (30). The solubility (log S) of selected ligands was implemented using the ESOL model (32, 33).

Results and Discussion

Molecular docking, as implemented through AutoDock 4.2, has emerged as a powerful technique for precisely identifying ligand-binding sites within proteins and elucidating the molecular interactions that promote stability in protein-ligand complexes. In molecular docking, the tasks of pose prediction and binding affinity prediction are complementary. Pose prediction involves generating a conformation that is subsequently evaluated based on the predicted binding affinity. Binding affinity characterizes the strength of the noncovalent interaction between a ligand and its receptor's binding site, with a higher binding affinity indicating a more robust and stable interaction, thus suggesting an increased likelihood of the ligand effectively influencing its biological activity. Docking programs generate multiple potential binding poses, each associated with a specific binding energy score. The optimal model is distinguished by the lowest (most negative) binding energy, signifying a more advantageous interaction. This investigation involved the evaluation of the AutoDock binding affinities of benzo[a]phenazin-5-ol derivatives A-L (Figure 1) (34) to determine their potential inhibitory activities on the C-kit kinase (Figure 2). The study utilized AutoDock 4.2 for molecular docking, wherein compounds A-L were docked into the C-kit kinase receptor, specifically the stem cell factor receptor with the PDB code 1t46, as illustrated in Figure 3.

[Downloaded from jabs.fums.ac.ir on 2026-11-10]
[DOI: 10.18502/jabs.v14i3.16359]



Ar: A = 3-$NO_2C_6H_4$, B = 2-$NO_2C_6H_4$, C = 4-$NO_2C_6H_4$, D = 2-ClC_6H_4, E = 3-ClC_6H_4, F = 3-ClC_6H_4, G = 3-FC_6H_4, H = 4-FC_6H_4, I = C_6H_5, J = 4-BrC_6H_4, K = 4-$OMeC_6H_4$, L = 4-$CO_2HC_6H_4$

Figure 1. Structures of benzo[a]phenazin-5-ol derivatives **A-L**.

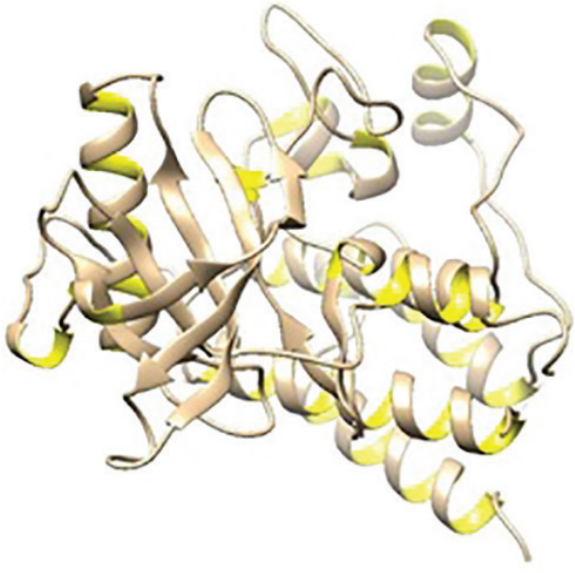


Figure 2. Structure of the protein C-Kit kinase receptor.

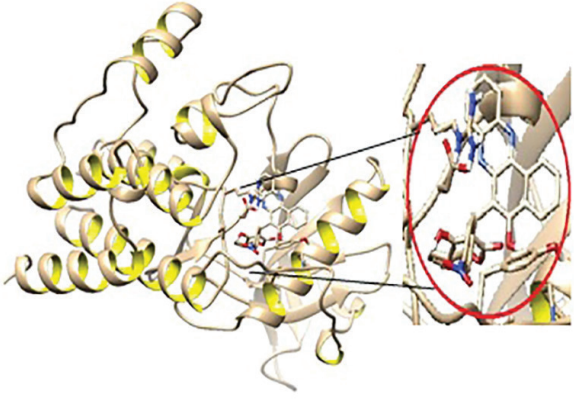


Figure 3. Docking of benzo[a]phenazine-5-ol derivative with C-Kit kinase.

To ensure the accuracy of the docking process, the bound inhibitor (Sunitinib) was assessed based on its proximity to the natively co-crystallized pose, with a maximum RMSD of 2.0 Å. Furthermore, the docked compounds were required to exhibit binding free energies (ΔGb) comparable to the native ligand and establish a significant number of hydrogen bonds with key amino acid Arg791(A) involved in the interaction between the inhibitor and C-kit kinase (1t46) (Table 1, Entry 1).

Benzo[a]phenazin-5-ol derivatives exhibited satisfactory binding free energies (ΔGb) when flexibly docked into the binding site of C-Kit kinase (PDB: 1t46) using AutoDock. Their binding affinities were comparable to those of the originally bound Sunitinib ligand (Table 1). The compounds demonstrated favorable binding poses, with binding free energies (ΔGb) ranging from -9.3 to -10.6 kcal/mol. These poses were characterized by RMSD values between 0.000 and 2.678 Å and involved 1-4 hydrogen bond interactions. Notably, the compounds exhibited greater binding affinities than Sunitinib, suggesting they may possess superior properties compared to the standard drug.

The interaction between receptor C-Kit and ligand A was characterized by the formation of strong bonds with three specific amino acids (Arg791(A), Ile789(A), His790(A)) via the oxygen atoms of nitro and hydroxy groups. These bonds formed hydrogen interactions within the active site of the receptor. The lengths of these hydrogen bonds with the receptor were measured at 2.58 Å, 2.93 Å, 3.14 Å, and 3.17 Å, respectively. It is noteworthy that both Sunitinib and compound A formed hydrogen bonds with the amino acid Arg791(A). Additionally, the calculated binding free energy was found to be -10.3 kcal/mol (Table 1, Entry 2).

Compound C, exhibiting the lowest energy level, established interactions with specific amino acids. The oxygen atoms of the nitro group formed strong bonds with Ile571(A) and Ile789(A) amino acids.

[Downloaded from jabs.fums.ac.ir on 2026-11-10]
[DOI: 10.18502/jabs.v14i3.16359]

Table 1. Binding free energies (ΔG_b), RMSD values, binding interactions and hydrogen bonds length of Sunitinib and new benzo[a]phenazine-5-ols docked into C-Kit kinase (PDB: 1t46).

Entry	Compound	Binding free energy (kcal/mol)	RMSD value	Binding Interaction (Amino acid residue)	Hydrogen bond length (Å)
1	Sunitinib	-6.9	4.714	Arg791(A)	3.10
2	**A**	-10.3	0.00	Ile789(A) Arg791(A) His790(A)	3.14 3.17 and 2.93 2.58
3	**B**	-10.3	2.428	-	-
4	**C**	-10.6	0.00	Ile789(A) Ile571(A)	3.07 2.99
5	**D**	-10.5	2.678	-	-
6	**E**	-10.2	0.00	-	-
7	**F**	-10.3	0.00	-	-
8	**G**	-10.2	2.665	Ile789(A)	3.04
9	**H**	-10.2	0.00	-	-
10	**I**	-10.1	0.00	-	-
11	**J**	-10.1	0.989	-	-
12	**K**	-9.3	0.00	-	-
13	**L**	-9.4	0.00	-	-

RMSD: Root Mean Square Deviation

The lengths of the hydrogen bonds with the receptor were measured at 2.99 Å and 3.07 Å, respectively, with a binding free energy of -10.6 kcal/mol (Table 1, Entry 4). Furthermore, compound G effectively aligned within the designated region of the C-Kit receptor and formed a single hydrogen bond with Ile789(A) through the oxygen atom of its hydroxy group. The length of this hydrogen bond with the receptor was measured at 3.04 Å, with a corresponding binding free energy of -10.2 kcal/mol (Table 1, Entry 8).

It was observed that most of the compounds were enveloped by hydrophobic amino acids, which occupied a considerable portion of the receptor space. This attribute is pivotal for their anticancer activity and underscores the potential of these benzo[a]phenazin-5-ol derivatives as promising candidates for C-kit kinase inhibition.

The RMSD provides valuable insights into the structural conformation of a protein and serves as an indicator of simulation equilibration. Moreover, analyzing the ligand RMSD (fit to protein) offers crucial information about the stability of the ligand in relation to the protein and its binding pocket. In a stable system, end-of-simulation fluctuations for small globular proteins typically range from 0-2 Å, with larger deviations indicating significant conformational changes. It was observed that the RMSD values of compounds **A** and **C** converged to a fixed value (0.00) towards the end of the simulation, indicating a stable conformation of the protein. The Ligplot results for Sunitinib and compounds **A**, **C**, **D**, and **G** are depicted in Figure 4. Furthermore, the docking results of all compounds were compared with those of a co-crystallized ligand and a standard inhibitor using ADME screening. This comparison likely offers valuable insights into the binding affinity and interactions of the hit compounds with the C-Kit kinase protein, relative to the known ligand Sunitinib.

The physicochemical properties of compounds **A-L** are detailed in Table 2. The drug-like properties of the compounds were evaluated according to Lipinski's rule of five, which includes criteria such as a molecular mass of less than 500 Da, no more than 5 hydrogen

[Downloaded from jabs.fums.ac.ir on 2026-11-10]
[DOI: 10.18502/jabs.v14i3.16359]

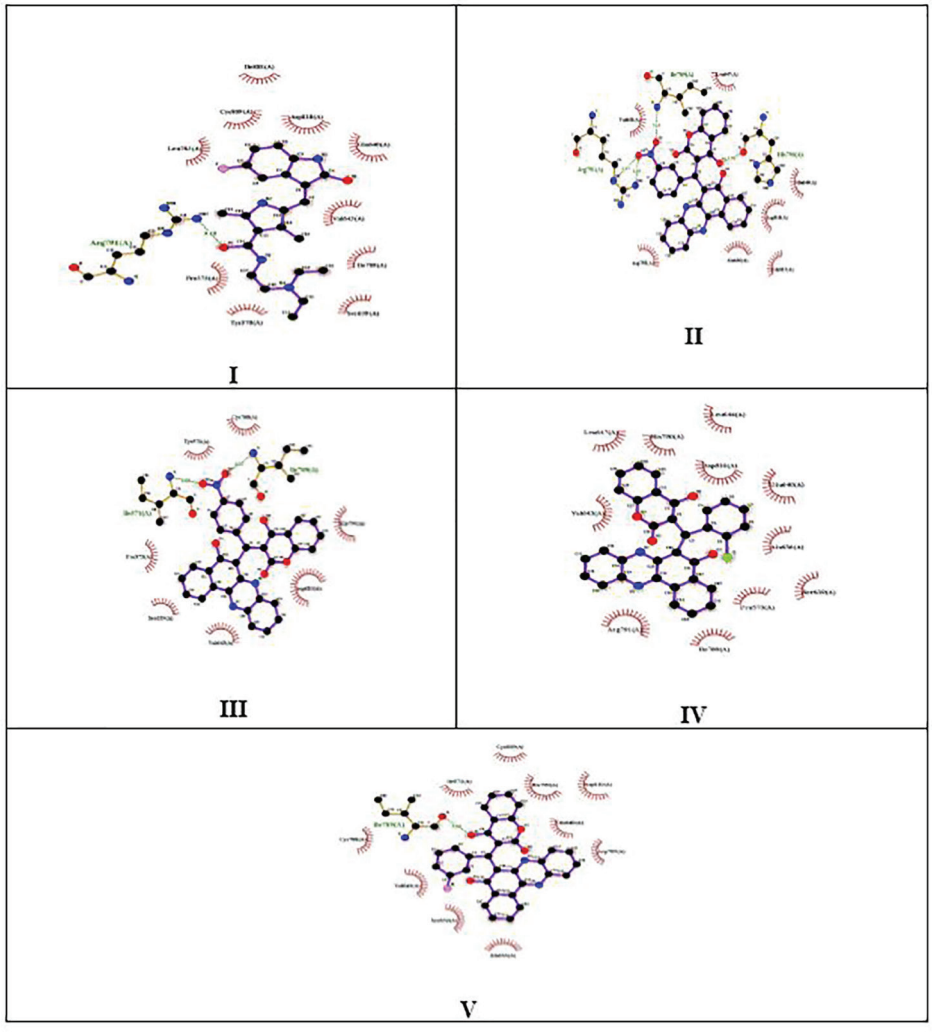


Figure 4. The ligplot results for: (**I**) Sunitinib 1-H bond with Arg791(A); (**II**) **A** forming 4-H bond with Arg791(A), IIe789(A), His790(A); (**III**) **C** forming 2-H bond with IIe571(A) and IIe789(A); (**IV**) **D** forming hydrophobic interactions; (**V**) **G** forming 1-H bond with IIe789(A).

bond donors, no more than 10 hydrogen bond acceptors, and an octanol-water partition coefficient of less than 5. The computed ADMET properties (gastrointestinal (GI) absorption; blood-brain barrier (BBB) permeation; inhibition of the cytochrome P450 system; permeability glycoprotein (P-gp) substrate) of the compounds are presented in Table 3. According to the results, all compounds exhibited low gastrointestinal absorption. All compounds, except for **C**, **D**, and **I**, were identified as potential substrates of P-gp. None of the compounds were predicted to inhibit cytochrome P450 (CYP) isoforms, indicating no potential inhibitory activity against these enzymes. Additionally, compounds **A**, **C**, **I**, and **K** each showed one violation of the Lipinski drug-likeness filters, while the other compounds exhibited two violations.

ADME screening helps identify compounds with unfavorable pharmacokinetic properties, thereby narrowing down the selection to more promising candidates. Our assay included these compounds to evaluate their potential as C-Kit kinase inhibitors through in silico studies. As a result, it was determined that compound **A** has the most pharmacological similarity with the Sunitinib drug and can be considered for further studies.

[Downloaded from jabs.fums.ac.ir on 2026-11-10]
[DOI: 10.18502/jabs.v14i3.16359]

Table 2. The physicochemical properties of compounds **A-L** and Sunitinib calculated with the SwissADME database.

Ligands	MW (g/mol)	nHA	nAHA	F.Csp^3	nRB	nHBA	nHBD	MR	TPSA (A^2)	Log s (ESOL)
Sunitinib	398.47	29	11	0.36	8	4	3	116.31	77.23	-3.72 Soluble
A	541.51	41	34	0.03	4	8	2	157.4	142.27	-7.38
B	541.51	41	34	0.03	4	8	2	157.4	142.27	-7.38
C	541.51	41	34	0.03	4	8	2	157.4	142.27	-7.38
D	530.96	39	34	0.03	3	6	2	153.59	96.45	-7.92
E	530.96	39	34	0.03	3	6	2	153.59	96.45	-7.92
F	530.96	39	34	0.03	3	6	2	153.59	96.45	-7.92
G	514.50	39	34	0.03	3	7	2	148.54	96.45	-7.48
H	514.50	39	34	0.03	3	7	2	148.54	96.45	-7.48
I	540.52	41	34	0.03	4	8	3	155.54	133.75	-7.19
J	575.41	39	34	0.03	3	6	2	156.28	96.45	-8.23
K	526.54	40	34	0.06	4	7	2	155.07	105.68	-7.39

MW: molecular weight; nHA: no. of heavy atom; nAHA: no. of arom. heavy atom; F.Csp^3: no. of sp^3 hybridized carbon out of total carbon count; nRB: no. of rotatable bonds; nHBA: no. of H-bond acceptors; nHBD: no. of H-bond donors, MR: molar refractivity; TPSA: topological polar surface area; ESOL: Estimated SOLubility.

Table 3. The bioavailability scores and pharmacokinetics of compounds **A-L** and Sunitinib calculated with SwissADME database.

Ligands	GI absorption	BBB permeant	P-gp inhibitor	CYP1A2 inhibitor	CYP2C19 inhibitor	CYP2C9 inhibitor	CYP2D6 inhibitor	CYP3A4 inhibitor	Log Kp (skin permeation) cm/s	Drug likeness Lipinski
Sunitinib	High	Yes	Yes	No	Yes	No	Yes	Yes	-6.86	Yes; 0 violation
A	Low	No	Yes	No	No	No	No	No	-5.28	Yes; 1 violation
B	Low	No	Yes	No	No	No	No	No	-5.28	Yes; 1 violation
C	Low	No	No	No	No	No	No	No	-5.28	Yes; 1 violation
D	Low	No	No	No	No	No	No	No	-4.65	No; 2 violations; MLOGP>4.15
E	Low	No	Yes	No	No	No	No	No	-4.65	No; 2 violations; MLOGP>4.15
F	Low	No	Yes	No	No	No	No	No	-4.65	No; 2 violations; MLOGP>4.15
G	Low	No	Yes	No	No	No	No	No	-4.92	No; 2 violations; MLOGP>4.15
H	Low	No	Yes	No	No	No	No	No	-4.92	No; 2 violations; MLOGP>4.15
I	Low	No	No	No	No	No	No	No	-5.49	Yes; 1 violation; MW>500
J	Low	No	Yes	No	No	No	No	No	-4.88	No; 2 violations; MLOGP>4.15
K	Low	No	Yes	No	No	No	No	No	-5.09	Yes; 1 violation

[Downloaded from jabs.fums.ac.ir on 2026-11-10]
[DOI: 10.18502/jabs.v14i3.16359]

Conclusions

This study aimed to explore the potential anticancer activities of various benzo[a]phenazin-5-ol derivatives through computational analysis, with a particular focus on their interactions with the C-kit kinase receptor. The AutoDock 4.2 study was performed to optimize the lead compounds. Upon molecular docking with the 1t46.PDB protein target, investigations revealed that compounds **A**, **C**, and **G** interacted with the C-Kit kinase through hydrogen bonds, whereas the remaining compounds interacted primarily through hydrophobic bonds. Notably, compounds **A** and **C** demonstrated the highest C-kit kinase inhibitory effects. The interaction energy analysis revealed that compounds **A** and **C** had significantly lower energy values compared to the Sunitinib ligand, indicating stronger binding affinities. Furthermore, the hydrogen bond lengths between compounds **A**, **C**, and amino acids were approximately 2.58-3.17 Å. The RMSD values for compounds **A** and **C** stabilized around 0.00, indicating a consistent protein conformation. According to the SwissADME results, while compound **A** outlined differences in pharmacokinetic properties compared to the Sunitinib drug, it adheres well to Lipinski's rules, suggesting good potential for absorption and distribution in the body. Thus, compound **A** appears to be a promising candidate for future drug design studies. Further research on its biological effects and mechanism of action is recommended to better understanding of its therapeutic potential.

Acknowledgments

The authors gratefully acknowledge for the assistance received from Imam Khomeini International University, Ghazvin, Iran.

Conflict of Interest

The authors declare no conflict of interest.

Funding

No financial support was provided relevant to this work.

Ethical Consideration

This computational work has been performed in compliance with all relevant ethical considerations.

Authors' Contribution

Abolfazl Olyaei: project design, conceptualization and drafting of main manuscript. Monir Shalbafan: docking and ADME analysis, review and editing. Fatemeh Rahimi: figures preparation and resources. Mahdieh Sadeghpour: supervision, analysis, editing and proofreading.

References

1 Wang S, Miller W, Milton J, Vicker N, Stewart A, Charlton P, et al. Structure–activity relationships for analogues of the phenazine-based dual topoisomerase I/II inhibitor XR11576. Bioorg Med Chem Lett. 2002; 12: 415-418.

2 Rewcastle GW, Denny WA, Baguley BC. Potential antitumor agents. 64. Synthesis and antitumor evaluation of dibenzo[1,4]dioxin-1-carboxamides: a new class of weakly binding DNA-intercalating agents. J Med Chem.1987; 30:843-851.

3 Gamage SA, Spicer JA, Rewcastle GW, Milton J, Sohal S, Dangerfield W, et al. Structure−Activity Relationships for Pyrido-, Imidazo-, Pyrazolo-, Pyrazino-, and Pyrrolophenazinecarboxamides as Topoisomerase-Targeted Anticancer Agents. J Med Chem. 2002; 45:740-743.

4 Vicker N, Burgess L, Chuckowree IS, Dodd R, Folkes AJ, Hardick DJ, et al. Novel Angular Benzophenazines: Dual Topoisomerase I and Topoisomerase II Inhibitors as Potential Anticancer Agents. J Med Chem. 2002; 45:721-739.

5 Olyaei A, Sadeghpour M. A review on lawsone-based benzo[a]phenazin-5-ol: Synthetic Approaches and Reactions. RSC Adv. 2022; 12: 13837-13895.

6 Lu G-p, Cai C. A One-pot, Efficient Synthesis of Polyfunctionalized Pyrido[2,3-*d*]pyrimidines and Uncyclized Adducts by Aldehydes, 1,3-Dicarbonyl Compounds, and 6-Aminouracils. J Heterocyclic Chem. 2014; 51: 1595-1602.

7 Kumari P, Bharti R, Parvin T. Synthesis of amino-uracil-tethered tri-substituted methanes in water by iodine-catalyzed multicomponent reactions. Mol

[Downloaded from jabs.fums.ac.ir on 2026-11-10]

[DOI: 10.18502/jabs.v14i3.16359]

Divers. 2019; 23: 205-213.
8 Safaei-Ghomi J, Pooramiri P, Babaei P. Green sono-synthesis of phenazinpyrimidines using CO_3O_4/ZnO@N-GQDs@SO_3H nanocomposite as a robust heterogeneous catalyst. J Chin Chem Soc. 2021; 68:1302-1309.
9 Kandhasamy S, Ramanathan G, Muthukumar T, Thyagarajan S, Umamaheshwari N, Santhanakrishnan VP, et al. Nanofibrous matrixes with biologically active hydroxybenzophenazine pyrazolone compound for cancer theranostics. Mater Sci Eng C. 2017; 74: 70-85.
10 Olyaei A, Aghajanzadeh A, Feizy E, Sadeghpour M. A green one-pot pseudo-five-component sequential protocol for the synthesis of novel 6,6′-(arylmethylene)bis(benzo[*a*]phenazin-5-ol) derivatives. J Chin Chem Soc. 2021; 68: 704-712.
11 Rahimi F, Olyaei A, Ghasemzadeh H. Multicomponent domino protocol for the one-pot synthesis of novel benzo[a]phenazin-5-ol derivatives. Res Chem Intermed. 2024; 50: 239-249.
12 Ashman LK. The biology of stem cell factor and its receptor C-kit. Int J Biochip Cell Biol. 1999; 31: 1037-1051.
13 Furitsu T, Tsujimura T, Tono T, Ikeda H, Kitayama H, Koshimizu U, et al. Identification of Mutations in the Coding Sequence of the Proto-oncogene c-kit in a Human Mast Cell Leukemia Cell Line Causing Ligand-independent Activation of c-kit Product. J Clin Invest. 1993; 92: 1736-1744.
14 Yavuz AS, Lipsky P E, Yavuz S, Metcalfe DD, Akin C. Evidence for the involvement of a hematopoietic progenitor cell in systemic mastocytosis from single-cell analysis of mutations in the c-kit gene. Blood. 2002; 100: 661-665.
15 Corless CL, Fletcher JA, Heinrich MC. Biology of gastrointestinal stromal tumors. J Clin Oncol. 2004; 22: 3813-3825.
16 Reith AD, Ellis C, Lyman SD, Anderson DM, Williams DE, Bernstein A, et al. Signal transduction by normal isoforms and W mutant variants of the Kit receptor tyrosine kinase. EMBO J. 1991; 10: 2451-2459.
17 Voytyuk O, Lennartsson J, Mogi A, Caruana G, Courtneidge S, Ashman LK, et al. Src family kinases are involved in the differential signaling from two splice-forms of c-Kit. J Biol Chem. 2003; 278: 9159-9166.
18 Maulik G, Bharti A, Khan E, Broderick RJ, Kijima T, Salgia R. Modulation of c-Kit/SCF Pathway Leads to Alterations in Topoisomerase-I Activity in Small Cell Lung Cancer. J Environ Pathol Toxicol. Oncol. 2004; 23: 237-251.
19 Pawson T. Protein modules and signalling networks. Nature. 1995; 373: 573-580.
20 Blume-Jensen P, Siegbahn A, Stabel S, Heldin CH, Rönnstrand L. Identification of the major phosphorylation sites for protein kinase C in kit/stem cell factor receptor in vitro and in intact cells. EMBO J. 1993; 12: 4199-4209.
21 Zhu WM, Dong W F, Minden M. Alternate splicing creates two forms of the human kit protein. Leuk Lymphoma. 1994; 12: 441-447.
22 Crosier PS, Ricciardi ST, Hall LR, Vitas MR, Clark SC, Crosier KE. Expression of isoforms of the human receptor tyrosine kinase c-kit in leukemic cell lines and acute myeloid leukemia. Blood. 1993; 82: 1151-1158.
23 Cheng H, Force T. Why do kinase inhibitors cause cardiotoxicity and what can be done about it? Prog Cardiovasc Dis. 2010; 53: 114-120.
24 Blay JY. Pharmacological management of gastrointestinal stromal tumours: an update on the role of sunitinib. Ann Oncol. 2010; 21: 208-215.
25 Liu Y-Z, Wang X-l, Wang X-y, Yu R-l, Liu D-q, Kang C-m. De novo design of VEGFR-2 tyrosine kinase inhibitors based on a linked-fragment approach. J Mol Model. 2016; 22: 222-230.
26 Gan HK, Seruga B, Knox JJ. Sunitinib in solid tumors. Expert Opin Invest Drugs. 2009; 18: 821-834.
27 Sanchez-Rodríguez EP, Santos-Lopez G, Cruz-Martínez H, Calaminici P, Medina DI. Pd_2 and CoPd dimers/N-doped graphene sensors with enhanced. Sensitivity for CO detection: A first-principles study. J Mol Model. 2023; 29: 252-260.
28 Muhammed MT, Yalcin EA. Molecular Docking: Principles, Advances, and Its Applications in Drug Discovery. Lett Drug Des Discov. 2022; 19: 757-768.
29 Elokely KM, Doerksen RJ. Docking challenge: protein sampling and molecular docking performance. J Chem Inf Model. 2013; 53: 1934-1945.
30 Daina A, Michielin O, Zoete V. SwissADME: a free web tool to evaluate pharmacokinetics, drug-likeness and medicinal chemistry friendliness of small molecules. Sci Rep. 2017; 7: 42717.
31 O'Boyle NM, Banck M, James CA, Morley C, Vandermeersch T, Hutchison GR. Open Babel: an open chemical toolbox. J Cheminform. 2011; 3: 33.
32 Delaney JS. ESOL: estimating aqueous solubility directly from molecular structure. J Chem Inf Model. 2004; 44: 1000-1005.
33 Ali J, Camilleri P, Brown MB, Hutt AJ, Kirton SB. Revisiting the general solubility equation: in silico

[Downloaded from jabs.fums.ac.ir on 2026-11-10]
[DOI: 10.18502/jabs.v14i3.16359]

prediction of aqueous solubility incorporating the effect of topographical polar surface area. J Chem Inf Model. 2012; 52: 420-428.

34 Rahimi F, Olyaei A, Ghasemzadeh H. Multicomponent domino protocol for the onepot synthesis of novel benzo[a]phenazin5ol derivatives. Res Chem Intermed. 2024; 50: 239-249.

[Downloaded from jabs.fums.ac.ir on 2026-11-10]

[DOI: 10.18502/jabs.v14i3.16359]